Configuration-Driven Unitary Group Approach for Generalized Van Vleck Variant Multireference Perturbation Theory†

Wanyi Jiang,‡ Yuriy G. Khait,‡,§ and Mark R. Hoffmann*,‡

Chemistry Department, University of North Dakota, Grand Forks, North Dakota 58202, and Russian Scientific Center "Applied Chemistry", St. Petersburg 197198, Russia

Received: December 15, 2008; Revised Manuscript Received: February 11, 2009

A new, efficient, configuration-driven algorithm utilizing the unitary group approach (UGA) was developed and implemented for the generalized van Vleck perturbation theory (GVVPT) variant of multireference perturbation theory. The computational speed has been improved by 1 or 2 orders of magnitude compared to the previous implementation based on the Table-CI technique. It is shown that the reformulation is applicable to both the second-order (GVVPT2) and third-order (GVVPT3) approximations. Calculations on model problems and on a chemically realistic description of cyclobutadiene are used to illustrate the performance of the method. The calculations on cyclobutadiene, using over 2.3 billion CSFs, provide results on geometric parameters and the barrier height of the automerization reaction in good agreement with established high accuracy results.

I. Introduction

Generalized van Vleck perturbation theory (GVVPT)[1−3] is distinguished from other multireference or quasidegenerate perturbation theories in that it is subspace-specific and allows for the interaction of the perturbed states of interest with the unperturbed complementary states. By using a degeneracy corrected reference state energy in the resolvent, as well as a hyperbolic tangent function as a switching function from nondegenerate to degenerate states, the notorious "intruder-state" problem is avoided completely. As a consequence, both ground and excited potential energy surfaces (PESs) generated by GVVPT are rigorously continuous and differentiable. GVVPT is also inherently spin-adapted; thus, it is capable of treating electronic states while maintaining a pure total spin quantum number. Reliable results have been obtained for a variety of difficult molecular systems, including difluorodioxirane,[4] azobenzenes,[5] etc., even at second order (GVVPT2), and GVVPT2 appears to be a promising method when large portions of PESs need to be considered at comparable levels of accuracy. However, the resolvent in the perturbation series in GVVPT is nonlinear and each external configuration needs to be handled explicitly. Because of the central role of configurations, the configuration-driven Table-CI technique[6,7] was selected for initial implementations of GVVPT methods to evaluate Hamiltonian matrix elements. Table-CI is not as efficient computationally as other modern CI methods, such as those based on the unitary group approach (UGA),[8−14] for the evaluation of matrix elements over configuration state functions (CSFs) or their products with trial vectors (i.e., the so-called sigma vectors). The UGA, especially graphical UGA (GUGA),[12−14] has usually been implemented in integral-driven, "loop-driven", or CSF-driven manners, which, while very efficient for CI calculations (especially those using a complete active space reference), is not well-suited for efficient use in GVVPT theory. For example, in our recent implementation of a GVVPT code based on a conventional CSF-based GUGA-CI program, blocks of Hamiltonian matrix elements were saved successively in fast memory and resorted implicitly to the corresponding external configurations. Although some improvements were found relative to the Table-CI variant, the enhancement of efficiency was limited. The situation deteriorates for larger molecular systems where the size of matrix blocks exceeds the available memory or not all CSFs of one external configuration are accessible with a reasonable partition size of the Hamiltonian matrix. A similar dilemma can be expected for other integral-driven or loop-driven algorithms.

In reality, a configuration-driven algorithm is not incompatible with the UGA technique. A combination of both has been realized efficiently in our recently developed multireference configuration interaction including single and double excitations (MRCISD) program,[15] which we refer to as CFGCI [i.e., configuration-driven (UGA)-CI]. In the new CFGCI program, calculation of sigma vectors is organized by a hierarchy of comparisons, starting from macroconfigurations (a set of configurations; see ref 16 for details), then configurations, and only finally CSFs. The narrowing of possibilities of interactions allows a significant reduction of conditional execution throughout the algorithm. Each macroconfiguration is represented by a modified distinct row table (mDRT), which is different from a regular DRT[8] in that it considers only the occupancies but ignores the spin of orbitals that have single occupancies. Thus, every viable path in a mDRT corresponds to one configuration, while in a regular DRT it represents one CSF. By using mDRTs, configurations are compared recursively to locate interacting configuration pairs, which identifies potentially nonvanishing Hamiltonian matrix elements. In practice, sets of related configurations can be processed simultaneously. Subsequently, the required integrals are retrieved and organized if necessary. Recombining the single orbital occupancies in the configuration and the precomputed branching spin diagram, the Shavitt step vectors[12] for each CSF in the configuration can be obtained and

† Part of the "George C. Schatz Festschrift".

* To whom correspondence should be addressed. E-mail: mhoffmann@chem.und.edu.

‡ University of North Dakota.

§ Russian Scientific Center "Applied Chemistry".

10.1021/jp811082p CCC: $40.75 © 2009 American Chemical Society
Published on Web 03/16/2009

the coupling coefficients evaluated by the UGA technique, specifically in our case, as proposed by Paldus and Boyle.[9]

To fully exploit the efficiency of GVVPT methods, GVVPT codes based on the configuration-driven algorithm with UGA techniques have been developed. In the new CFGCI-based GVVPT, interactions of each external configuration with all model configurations are conveniently considered together for both eigenvectors ($\mathbf{X}$) and sigma vectors ($\boldsymbol{\sigma} = \mathbf{HX}$). All coupling coefficients are calculated "on the fly", so there is no external "formula file" and correspondingly very little I/O or memory requirement. Although Hamiltonian matrix elements are evaluated twice, to minimize memory usage and/or bandwidth usage, the overall speed-up relative to the original Table-CI-based algorithm is several orders of magnitude. Furthermore, memory usage is not a significant concern for GVVPT2, since the largest memory requirement in GVVPT2 is the storage of a small subset of the two-electron integrals, which scales as a^2k^2 for a active orbitals and k external orbitals. With modern computers having at least 2 gigabytes of memory per processor, this allows calculations of molecular systems with 20 active orbitals and up to 1000 external orbitals to be performed on a single node. In practice, it has been found that the computation time of the new GVVPT2 code is much less than that of the preceding multiconfiguration self-consistent field (MCSCF) in some large cases. Although we make no claims of particularly fast MCSCF code, on account of our rigorous control of Hessian eigenvalue structure, the code should be considered to be a modern, production caliber MCSCF code. Our main goal in this Article is to give a detailed account of the configuration-driven algorithm of UGA-based GVVPT.

In third-order GVVPT (GVVPT3), the total energies include *all orders* of energy corrections based on the first-order primary−external space ($P-Q$) interactions, which are calculated in GVVPT2. GVVPT3 has been demonstrated to be a close approximation to MRCISD, and the computation effort is equivalent to one iteration of MRCISD.[17]

Some test calculations have been performed for different GVVPT2 and GVVPT3 codes, and the computation times are compared with the earlier Table-CI-based algorithm. While the speed of GVVPT3 code depends linearly on its parent MRCISD code, the efficiency of the new GVVPT2 code, based on the CFGCI algorithm, has been greatly improved relative to previous code. To demonstrate the efficiency of the new GVVPT2 code, results from a number of diatomics are analyzed and cyclobutadiene (c-C_4H_4), which is computationally unfeasible (with chemically reasonable basis sets and model space) with the older code, has been studied in greater detail to provide a concrete example. The truncated model space of c-C_4H_4 includes 3094 CSFs and the total space is spanned by 2 389 313 884 CSFs when using the cc-pVTZ basis set. The GVVPT2 part in a single point calculation took only 314 s on a 2.0 GHz dual core AMD Opteron Processor 2212. Although chemical results are not the primary focus of this Article, we compared the results of calculations on c-C_4H_4 with previous high accuracy results. It was found that the predicted geometries of the rectangular ground-state and square transition structure of c-C_4H_4 are in good agreement with those obtained by the MRAQCC method.[18] The energy barrier height for the automerization reaction of c-C_4H_4 is predicted to be 7.7 kcal/mol, which is close to the 8.6 kcal/mol predicted by MRAQCC.

The Article is organized as follows. A section on theoretical background, in which the parts of the GVVPT2 and GVVPT3 formalisms that are needed to understand the UGA implementation are given, is presented. Then, the configuration-driven algorithms for GVVPT2 and GVVPT3 are given in detail. Some test examples are collected and discussed. The conclusions are given in a final section.

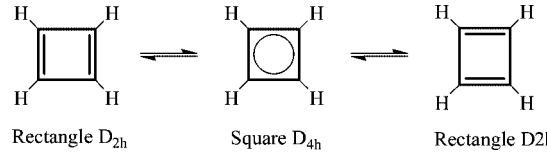

Figure 1. Automerization of cyclobutadiene.

II. Theoretical Background

In GVVPT, the total Hilbert space $\boldsymbol{L}$ is spanned by an orthonormal set of N CSFs

$$\boldsymbol{L} = \mathrm{Span}\{F_n\}_{n=1}^{N}$$

It is partitioned into a model space $\boldsymbol{L}_M$, often of a CASSCF type but more generally of a MCSCF type with additional restrictions on occupancies of orbital groups, and an external space $\boldsymbol{L}_Q$ (whose configurations are related to the model ones through excitations to external orbitals)

$$\boldsymbol{L}_M = \mathrm{Span}\{F_m\}_{m=1}^{N_m}$$

$$\boldsymbol{L}_Q = \mathrm{Span}\{F_q\}_{q=1}^{N_q}$$

The primary subspace $\boldsymbol{L}_P \subset \boldsymbol{L}_M$, with dimension $N_p = \dim(L_P)$, is spanned by the N_p lowest orthonormal eigenvectors, $\{\Phi_p\}_{p=1}^{N_p}$, of the unperturbed Hamiltonian in the model space

$$\langle \Phi_p | H | \Phi_p \rangle = \mathbf{E}_p^{(0)} \tag{1}$$

where $\mathbf{E}_p^{(0)} = \mathrm{diag}\{E_1^{(0)}, E_2^{(0)},..., E_{N_p}^{(0)}\}$ is a diagonal matrix with energies of the unperturbed primary states. The set $|\boldsymbol{\Phi}_P\rangle = |\Phi_1, \Phi_2,..., \Phi_{N_p}\rangle$ is connected with the many-electron basis set $\mathbf{F}_M = |F_1, F_2,..., F_{N_m}\rangle$ through a transformation matrix $\mathbf{C}_{MP}$

$$|\boldsymbol{\Phi}_P\rangle = |\mathbf{F}_M\rangle \mathbf{C}_{MP} \tag{2}$$

which satisfies the equations

$$\mathbf{H}_{MM}\mathbf{C}_{MP} = \mathbf{C}_{MP}\mathbf{E}_P^{(0)} \qquad (\mathbf{H}_{MM} = \langle \mathbf{F}_M | \hat{H} | \mathbf{F}_M \rangle) \tag{3}$$

$$\mathbf{C}_{MP}^{\dagger}\mathbf{C}_{MP} = \mathbf{I}_P \tag{4}$$

If the molecular orbitals were optimized in an MCSCF calculation, with the same group and occupancy structure as the model space, one can recognize the primary space as the set of N_p lowest MCSCF states.

Let us introduce the projectors $\hat{P}_M = |\mathbf{F}_M\rangle\langle\mathbf{F}_M|$ and $\hat{P} = |\boldsymbol{\Phi}_P\rangle\langle\boldsymbol{\Phi}_P|$ on the model and primary subspaces, respectively. Then, the projector $\hat{S} = \hat{P}_M - \hat{P}$ will be a projector on the complementary (secondary) subspace $\boldsymbol{L}_S$ ($\boldsymbol{L}_P \oplus \boldsymbol{L}_S = \boldsymbol{L}_M$), and the following conditions will be satisfied

$$\hat{P}\hat{H}\hat{P} = |\boldsymbol{\Phi}_P\rangle E_P^{(0)} \langle \boldsymbol{\Phi}_P| \tag{5}$$

$$\hat{S}\hat{H}\hat{P} = 0 \tag{6}$$

$$\hat{P}\hat{H}\hat{S} = 0 \tag{7}$$

$$\hat{P}\hat{H}\hat{P} + \hat{S}\hat{H}\hat{S} = \hat{P}_M\hat{H}\hat{P}_M \tag{8}$$

In the framework of the GVVPT2 method, the effective Hamiltonian matrix within the model space is defined as follows

$$\hat{P}\hat{H}^{\text{eff}}\hat{P} = \hat{P}\hat{H}\hat{P} + \frac{1}{2}\hat{P}[\hat{H}\hat{X}^{(1)} + (\hat{X}^{(1)})^{\dagger}\hat{H}]\hat{P} \tag{9}$$

$$\hat{S}\hat{H}^{\text{eff}}\hat{P} = \hat{S}\hat{H}\hat{X}^{(1)}\hat{P} \tag{10}$$

$$\hat{P}\hat{H}^{\text{eff}}\hat{S} = \hat{P}\hat{X}^{(1)+}\hat{H}\hat{S} \tag{11}$$

$$\hat{S}\hat{H}^{\text{eff}}\hat{S} = \hat{S}\hat{H}\hat{S} \tag{12}$$

where $\hat{X}^{(1)} = -(\hat{X}^{(1)})^{\dagger}$ and $\hat{X}^{(1)} = \hat{Q}\hat{X}^{(1)}\hat{P} - \hat{P}(\hat{X}^{(1)})^{\dagger}\hat{Q}$.

Although the definition of the complementary subspace coincides with that in the intermediate Hamiltonian approaches,[19] GVVPT describes its interaction with $\boldsymbol{L}_Q$ in a completely different way, i.e., through coupling through the primary space (see eqs 10 and 11 for GVVPT2 and eq 28 for GVVPT3). It is this feature that allows facile avoidance of intruder states as well as high efficiency algorithms. The most straightforward definition of the elements of the matrix $\mathbf{X}^{(1)}_{QP}$ is

$$X^{(1)}_{qi} = \frac{\langle F_q|H|\Phi_i\rangle}{\varepsilon^{(0)}_i - \varepsilon^i_q} \qquad (i \in P, q \in Q) \tag{13}$$

where $\varepsilon^{(0)}_i$ and ε^i_q are Møller−Plesset-type energies, which are computed from the state-specific one-particle reduced density matrix $\mathbf{D}^i$

$$D^i_{ab} = \langle\Phi_i|E_{ab}|\Phi_i\rangle = \sum_{mn} C_{mi}C_{ni}\langle F_m|E_{ab}|F_n\rangle \tag{14}$$

($m, n \in M$, $i \in P$ and a, b are occupied orbitals), and state-dependent orbital energies f^i_μ

$$f^i_\mu = h_{\mu\mu} + \sum_{a\geq b} D^i_{ab}[(\mu\mu|ab) - \frac{1}{2}(\mu a|\mu b)] \tag{15}$$

($i \in P$ and a, b are occupied orbitals; μ is any orbital).

Finally, $\varepsilon^{(0)}_i$ and ε^i_q are obtained

$$\varepsilon^{(0)}_i = \sum_a f^i_a D^i_{aa} \tag{16}$$

$$\varepsilon^i_q = \sum_\mu f^i_\mu N^q_\mu \qquad (=\varepsilon^i_{\mathbf{e}}) \tag{17}$$

ε^i_q is the state-specific zeroth-order energy of CSF q, which has the same value for all external CSFs belonging to a given external configuration ($\mathbf{e}$), and N^q_μ is the occupation number of orbital μ in CSF q.

The straightforward definition of zeroth-order energy described above often leads to small or even sign-reversed denominators. The GVVPT method adjusts (or shifts) the zeroth-order energy differences by two considerations. Following degeneracy corrected perturbation theory for single determinants, the reference energy is lowered and the energy difference between $\varepsilon^{(0)}_i$ and ε^i_q is calculated in the following way

$$\Delta_i = \frac{1}{2}(\varepsilon^i_q - \varepsilon^{(0)}_i) + \frac{1}{2}\sqrt{(\varepsilon^i_q - \varepsilon^{(0)}_i)^2 + 4\sum_{q\in\mathbf{e}} H^2_{qi}} \tag{18}$$

which considers the quasidegeneracy of the CSFs within each external configuration. Second, a hyperbolic tangent function is applied to provide a meaningful bound when the energy difference Δ_i approaches zero. The hyperbolic tangent acts as a switching function from nondegenerate to degenerate perturbation theory. Thus, the final form for the GVVPT2 coefficients is

$$X^{(1)}_{qi} = \frac{-\tanh(\Delta_i)}{\Delta_i}H_{qi} = \frac{-\tanh(\Delta_i)}{\Delta_i}\sum_{m\in M} H_{qm}C_{mi} \tag{19}$$

A representation of the effective Hamiltonian matrix in the basis, $|\mathbf{F}_M\rangle$, of the model space can be written as

$$\begin{aligned}\hat{P}_M\hat{H}^{\text{eff}}\hat{P}_M &= \hat{P}\hat{H}^{\text{eff}}\hat{P} + \hat{P}\hat{H}^{\text{eff}}\hat{S} + \hat{S}\hat{H}^{\text{eff}}\hat{P} + \hat{S}\hat{H}^{\text{eff}}\hat{S}\\ &= \hat{P}_M\hat{H}\hat{P}_M + \hat{P}(\hat{X}^{(1)})^{\dagger}\hat{H}\hat{P}_M + \hat{P}_M\hat{H}\hat{X}^{(1)}\hat{P} -\\ &\quad \frac{1}{2}\hat{P}(\hat{H}\hat{X}^{(1)} + (\hat{X}^{(1)})^{\dagger}\hat{H})\hat{P}\end{aligned} \tag{20}$$

In block matrix form, the above equation can be written as

$$\begin{aligned}\mathbf{H}^{\text{eff}}_{MM} = \mathbf{H}_{MM} + (\mathbf{HX})_{MP}\mathbf{C}^{\dagger}_{PM} + \mathbf{C}_{MP}(\mathbf{HX})^{\dagger}_{PM} -\\ \mathbf{C}_{MP}(\mathbf{CHX})_{PP}\mathbf{C}^{\dagger}_{PM}\end{aligned} \tag{21}$$

where $\mathbf{C}_{MP}$ are the eigenvectors of the unperturbed model Hamiltonian matrix, and

$$(\mathbf{HX})_{MP} = \mathbf{H}_{MQ}\mathbf{X}_{QP} \tag{22}$$

$$(\mathbf{CHX})_{PP} = \frac{1}{2}[\mathbf{C}^{\dagger}_{PM}(\mathbf{HX})_{MP} + (\mathbf{HX})^{\dagger}_{PM}\mathbf{C}_{MP}] \tag{23}$$

The diagonalization of the effective Hamiltonian matrix can be performed directly using a transformation technique or by Davidson's method[20] for larger model spaces. Instead of storing the entire effective Hamiltonian matrix, the contributions to sigma vectors from the GVVPT2 corrections are evaluated directly in each iteration. This approach allows large model spaces to be considered. The $\boldsymbol{\sigma}$ vectors for the Davidson diagonalization are evaluated as follows

$$\begin{aligned}\boldsymbol{\sigma}_{MR} &= \mathbf{H}^{\text{eff}}_{MM}\mathbf{B}_{MR}\\ &= \mathbf{H}_{MM}\mathbf{B}_{MR} + (\mathbf{HX})_{MP}(\mathbf{C}^{\dagger}_{PM}\mathbf{B}_{MR})_{PR} +\\ &\quad \mathbf{C}_{MP}[(\mathbf{HX})^{\dagger}_{PM}\mathbf{B}_{MR} - (\mathbf{CHX})_{PP}(\mathbf{C}^{\dagger}_{PM}\mathbf{B}_{MR})_{PR}]\end{aligned} \tag{24}$$

where $\mathbf{B}_{MR}$ are the trial vectors for the Davidson diagonalization. Since the unperturbed model Hamiltonian matrix is sparse, it is computationally more advantageous to form $\boldsymbol{\sigma}$ vectors directly from the unperturbed model Hamiltonian matrix and the corrections without the explicit construction of the effective Hamiltonian matrix.

GVVPT3 energies include all orders of energy corrections based on the first-order $P-Q_1$ interaction. The effective Hamiltonian is defined as

$$\hat{\mathrm{H}}_U^{\mathrm{eff}} = (e^{-X^{(1)}})\hat{H}(e^{X^{(1)}}) \tag{25}$$

where $X^{(1)}$ has been obtained previously in GVVPT2. GVVPT3 energies can be obtained by diagonalizing the effective Hamiltonian matrix

$$\hat{P}_M\hat{H}_U^{\mathrm{eff}}\hat{P}_M = \hat{P}\hat{H}_U^{\mathrm{eff}}\hat{P} + \hat{P}\hat{H}_U^{\mathrm{eff}}\hat{S} + \hat{S}\hat{H}_U^{\mathrm{eff}}\hat{P} + \hat{S}\hat{H}_U^{\mathrm{eff}}\hat{S} \tag{26}$$

The terms on the right side of above equation can be expanded

$$\hat{P}\hat{H}_U^{\mathrm{eff}}\hat{P} = \hat{P}e^{-X^{(1)}}(\hat{P} + \hat{Q})\hat{H}(\hat{P} + \hat{Q})e^{X^{(1)}}\hat{P} \tag{27}$$

$$\hat{P}\hat{H}_U^{\mathrm{eff}}\hat{S} = \hat{P}e^{-X^{(1)}}\hat{Q}\hat{H}(\hat{P}_M - \hat{P}) \tag{28}$$

$$\hat{S}\hat{H}_U^{\mathrm{eff}}\hat{S} = \hat{S}\hat{H}\hat{S} \tag{29}$$

Explicit determination of the secondary space eigenvectors can be circumvented, and the effective Hamiltonian expanded in the basis of the model space can be written as

$$\begin{aligned}\hat{P}_M\hat{H}_U^{\mathrm{eff}}\hat{P}_M = {} & \hat{P}_M\hat{P}e^{-X^{(1)}}\hat{P}\hat{H}\hat{P}e^{X^{(1)}}\hat{P}\hat{P}_M + \\ & \hat{P}_M\hat{P}e^{-X^{(1)}}\hat{Q}\hat{H}\hat{P}e^{X^{(1)}}\hat{P}\hat{P}_M + \hat{P}_M\hat{P}e^{-X^{(1)}}\hat{P}\hat{H}\hat{Q}e^{X^{(1)}}\hat{P}\hat{P}_M + \\ & \hat{P}e^{-X^{(1)}}\hat{Q}\hat{H}\hat{Q}e^{X^{(1)}}\hat{P}\hat{P}_M + \hat{P}_M\hat{P}e^{-X^{(1)}}\hat{Q}\hat{H}\hat{P}_M - \\ & \hat{P}_M\hat{P}e^{-X^{(1)}}\hat{Q}\hat{H}\hat{P}\hat{P}_M + \hat{P}_M\hat{H}\hat{Q}e^{X^{(1)}}\hat{P} - \hat{P}_M\hat{P}\hat{H}\hat{Q}e^{X^{(1)}}\hat{P}\hat{P}_M + \\ & \hat{P}_M\hat{H}\hat{P}_M - \hat{P}_M\hat{P}\hat{H}\hat{P}\hat{P}_M\end{aligned} \tag{30}$$

In the matrix form, the effective Hamiltonian is

$$\begin{aligned}(\mathbf{H}_U^{\mathrm{eff}})_{MM} = {} & \mathbf{C}_{MP}\mathbf{U}_{PP}^{\dagger}\mathbf{H}_{PP}\mathbf{U}_{PP}\mathbf{C}_{PM}^{\dagger} + \\ & \mathbf{C}_{MP}\mathbf{V}_{PP}^{\dagger}\mathbf{X}_{PQ}^{\dagger}\mathbf{H}_{QP}\mathbf{U}_{PP}\mathbf{C}_{PM}^{\dagger} + \mathbf{C}_{MP}\mathbf{U}_{PP}^{\dagger}\mathbf{H}_{PQ}\mathbf{X}_{QP}\mathbf{V}_{PP}\mathbf{C}_{PM}^{\dagger} + \\ & \mathbf{C}_{MP}\mathbf{V}_{PP}^{\dagger}\mathbf{X}_{PQ}^{\dagger}\mathbf{H}_{QQ}\mathbf{X}_{QP}\mathbf{V}_{PP}\mathbf{C}_{PM}^{\dagger} + \mathbf{C}_{MP}\mathbf{V}_{PP}^{\dagger}\mathbf{X}_{PQ}^{\dagger}\mathbf{H}_{QM} - \\ & \mathbf{C}_{MP}\mathbf{V}_{PP}^{\dagger}\mathbf{X}_{PQ}^{\dagger}\mathbf{H}_{QP}\mathbf{C}_{PM}^{\dagger} + \mathbf{H}_{MQ}\mathbf{X}_{QP}\mathbf{V}_{PP}\mathbf{C}_{PM}^{\dagger} - \\ & \mathbf{C}_{MP}\mathbf{H}_{PQ}\mathbf{X}_{QP}\mathbf{V}_{PP}\mathbf{C}_{PM}^{\dagger} + \mathbf{H}_{MM} - \mathbf{C}_{MP}\mathbf{H}_{PP}\mathbf{C}_{PM}^{\dagger}\end{aligned} \tag{31}$$

where $\mathbf{U}_{PP} = (e^{\mathbf{X}^{(1)}})_{PP}$ and $\mathbf{V}_{PP}$ is defined by

$$(e^{\mathbf{X}^{(1)}})_{QP} = \mathbf{X}_{QP}^{(1)}\mathbf{V}_{PP} \tag{32}$$

The matrices $\mathbf{U}_{PP}$ and $\mathbf{V}_{PP}$ can be obtained easily from the eigenvalues and eigenvectors of the small (i.e., $N_p \times N_p$) matrix $\mathbf{A}_{PP} = \mathbf{X}_{PQ}^{\dagger}\mathbf{X}_{QP}$

$$\mathbf{A}_{PP} = \mathbf{T}_{PP}\mathbf{D}_P^2\mathbf{T}_{PP}^{\dagger} \qquad (\mathbf{T}_{PP}^{\dagger} = \mathbf{T}_{PP}^{-1}) \tag{33}$$

Then

$$\mathbf{U}_{PP} = (e^{\mathbf{X}^{(1)}})_{PP} = (\cosh \mathbf{X}^{(1)})_{PP} = \mathbf{T}_{PP}\cos \mathbf{D}_P\mathbf{T}_{PP}^{\dagger} \tag{34}$$

$$\mathbf{V}_{PP} = \mathbf{T}_{PP}(\mathbf{D}_P^{-1}\sin \mathbf{D}_P)\mathbf{T}_{PP}^{\dagger} \tag{35}$$

Finally, the $\boldsymbol{\sigma}$ vectors for the Davidson diagonalization are evaluated as follows

$$\begin{aligned}\boldsymbol{\sigma}_{MR} = {} & (\mathbf{H}_U^{\mathrm{eff}})_{MM}\mathbf{B}_{MR} \\ = {} & \mathbf{H}_{MM}\mathbf{B}_{MR} + \mathbf{C}_{MP}(\mathbf{Y}_{PP}(\mathbf{C}_{PM}^{\dagger}\mathbf{B}_{MR})_{PR} + \\ & (\mathbf{Z}_{PM}^{\dagger}\mathbf{B}_{MR})_{PR}) + \mathbf{Z}_{MP}(\mathbf{C}_{PM}^{\dagger}\mathbf{B}_{MR})_{PR}\end{aligned} \tag{36}$$

where

$$\begin{aligned}\mathbf{Y}_{PP} = {} & \mathbf{U}_{PP}^{\dagger}\mathbf{E}_P\mathbf{U}_{PP} - \mathbf{E}_P + (\mathbf{HXV})_{PP}^{\dagger}\mathbf{U}_{PP} + \\ & \mathbf{U}_{PP}^{\dagger}(\mathbf{HXV})_{PP} + \mathbf{V}_{PP}^{\dagger}(\mathbf{XHX})_{PP}\mathbf{V}_{PP} - (\mathbf{HXV})_{PP}^{\dagger} - (\mathbf{HXV})_{PP}\end{aligned} \tag{37}$$

$$\mathbf{Z}_{MP} = (\mathbf{HXV})_{MP} \tag{38}$$

From a computational perspective, the most time-consuming part of GVVPT3 is the evaluation of matrix **XHX**, which is equivalent to one iteration of MRCISD in computation time.

III. Computational Implementation

The most time-consuming step in GVVPT2 is the evaluation of the correction to the wave function, $\mathbf{X}_{QP}$, and subsequently the sigma vector $(\mathbf{HX})_{MP}$. A computational difficulty is that the value of any X_{qp} for a given CSF (q) is only available after evaluation of H_{qi} for all CSFs belonging to one external configuration ($q \in \mathbf{e}$). Thus, an efficient code requires an explicit treatment of configurations, which is essentially unavailable from conventional GUGA-CI codes based on integral-driven or loop-driven algorithms. Moreover, once the values of X_{qp} are available for all $q \in \mathbf{e}$, $(HX)_{mi}$ is evaluated, which requires the matrix element H_{qm} once again. In principle, it is possible to save the values of H_{qm} for all $q \in \mathbf{e}$ in memory, or on disk, for the evaluation of $(HX)_{mi}$. However, there are some drawbacks in doing so. First, the matrix $\mathbf{H}_{QM}$ is sparse, with a nonzero pattern that is not readily amenable to sparse storage techniques; storage of the entire matrix causes unnecessary calculations. Second, for large calculations, the number of nonzero matrix elements of $\mathbf{H}_{QM}$ could easily exceed the available fast memory space. Temporary storage on disk is not generally viable, since I/O operations on large disk files are slow, especially when the writing and reading are interspersed. An alternative is to recalculate the matrix element H_{qm} during the evaluation of $(HX)_{mp}$. In this case, memory usage is minimized and most significant usage is for the storage of two-electron integrals, which scales as a^2k^2 for a active orbitals and k external orbitals for GVVPT2. Since the implementation of the new GVVPT2 code, very large calculations have been applied without any memory issue; e.g., a large calculation with 33 153 model CSFs and over 18 billion total CSFs was performed and completed successfully.

It is clear that when the denominator Δ_i in eq 19 approaches zero, numerical instabilities are a possibility and there is need for simultaneous consideration of numerator and denominator. In particular, one can set $X_{qi} \equiv -H_{qi}$, when the absolute value of Δ_i is smaller than a certain threshold, e.g., 10^{-7}.

Following the CFGCI algorithm,[15] the evaluation of $\mathbf{X}_{QP}$ and $(\mathbf{HX})_{MP}$ starts with macroconfigurations, which are sets of mathematically well-defined configurations.[16] The details of the generation of configurations from a compact mDRT representation of macroconfigurations will be discussed in a separate publication.[15] The orbitals are partitioned into core orbitals that are always doubly occupied in all configurations, virtual orbitals that are always empty in all configurations, internal orbitals that have a nonzero occupancy in at least one reference (model) configuration, and external orbitals that are empty in reference (model) configurations, but can have a nonzero occupancy in excited (external) configurations. While the treatment of the first two kinds of orbitals is trivial, the internal and external orbitals are handled separately for the sake of efficiency.[21]

The algorithms for GVVPT2 and GVVPT3 are given in detail below. The superscript on $X_{qi}^{(1)}$ indicating first-order $P-Q_1$ interactions is dropped for clarity.

(0) Initialization: memory allocations, etc.
(1) Calculate diagonal elements of the model Hamiltonian matrix H_{mm} ($m \in [1, N_m]$). Calculate the off-diagonal elements in matrix $\mathbf{H}_{MM}$ and store the nonzero elements. Diagonalize $\mathbf{H}_{MM}$ to obtain the model CI vectors $\mathbf{C}_{MP}$ and energies of the primary states, $E_p^{(0)}$, $p \in [1, N_p]$.
(2) Calculate the one-particle reduced density matrices for all states, D_{ab}^i, the orbital energies, f_μ^i, and the zeroth-order primary state energy, $\varepsilon_i^{(0)}$, as defined by a conventional, Møller−Plesset-type, one-electron Hamiltonian for each primary state.
(3) Calculate the GVVPT2 first-order corrections, $\mathbf{X}_{qi}$, and matrix $(\mathbf{HX})_{mi} = \sum_{q\in Q} \langle F_m|\hat{H}|F_q\rangle X_{qi}$ and $(\mathbf{X}^\dagger\mathbf{X})_{ij} = \sum_{q\in Q} X_{iq}^\dagger X_{qj}$.
  (3.1) Initialize $(\mathbf{HX})_{MP}$, $\mathbf{X}_{QP}$ ($\mathbf{H}_{QP}$), and $(\mathbf{X}^\dagger\mathbf{X})_{PP}$.
  (3.2) Loop over external (Q-) macroconfigurations
    Loop over Q_{int}-configurations (occupancies in internal orbitals)
    Loop over all interacting model (M-) macroconfigurations
    Loop over model (M-) configurations
    If the model configuration interacts with the Q_{int}-configuration
    If X_{QP} is being evaluated:
    Calculate $\mathbf{H}_{qi} = \sum_{m\in M} \langle F_q|\hat{H}|F_m\rangle C_{mi}$;
    else if $(\mathbf{HX})_{MP}$ is being evaluated:
    Calculate $(\mathbf{HX})_{mi} = \sum_{q\in Q} \langle F_m|\hat{H}|F_q\rangle X_{qi}$
    (next M-configuration)
    (next M-macroconfiguration)
    If X_{QP} is being evaluated:
    Loop over Q-configurations (all possible occupancies in external orbitals)
    Calculate elements in $\mathbf{X}_{QP}$
    Calculate ε_q^i and Δ_i
    If $|\Delta_i| <$ threshold, $\mathbf{X}_{qi} = -H_{qi}$;
    else $X_{qi} = [-\tanh(\Delta_i)/\Delta_i]H_{qi}$
    Calculate $(\mathbf{X}^\dagger\mathbf{X})_{ij}$
    Go to loop over all interacting M-macroconfigurations to evaluate $(\mathbf{HX})_{MP}$;
    else
    Reinitialize $\mathbf{X}_{QP}$ ($\mathbf{H}_{QP}$)
    Go to next Q_{int}-configuration to evaluate $\mathbf{X}_{QP}$
(4) Calculate $(\mathbf{CHX})_{PP}$ and diagonalize the GVVPT2 effective Hamiltonian matrix $\mathbf{H}_{MM}^{\text{eff}}$, which is not explicitly constructed, using Davidson's method with $\boldsymbol{\sigma}$ vectors as in eq 24.
(5) The primary−primary effective Hamiltonian matrix could also be built and diagonalized (this can be useful for direct comparison with multistate CASPT2 and MCQDPT).
  (5.1) Calculate $\mathbf{H}_{PP}^{\text{eff}} = (\mathbf{CHX})_{PP} + \mathbf{E}_P^{(0)}$.
  (5.2) Diagonalize $\mathbf{H}_{PP}^{\text{eff}}$ to obtain the eigenvalues and eigenvectors.
  Since GVVPT3 uses the same first-order corrections generated for GVVPT2, the above algorithm for GVVPT2 is executed with the addition of a few more steps.
(6) Calculate $(\mathbf{X}^+\mathbf{HX})_{PP}$
  (6.1) Initialize $(\mathbf{HX})_{QP}$
  (6.2) Loop over bra Q-macroconfigurations
    Loop over ket Q-macroconfigurations
    If two macroconfigurations interact,
    Loop over bra Q_{int}-configurations
    Loop over ket Q_{int}-configurations
    If two configurations interact,
    Needed integrals are gathered from the whole array and organized.
    Coupling coefficients are evaluated.
    Loop over viable configurations for external orbitals.
    Evaluate $(\mathbf{HX})_{qi} = \sum_{q,q'\in Q} \langle F_q|\hat{H}|F_{q'}\rangle X_{q'i}$
    (next ket Q_{int}-configuration)
    (next bra Q_{int}-configuration)
    (next ket Q-macroconfiguration)
    (next bra Q-macroconfiguration)
  (6.3) Calculate $(\mathbf{XHX})_{ij} = \sum_{q\in Q} X_{qi}(HX)_{qj}$.
(7) Diagonalize $\mathbf{X}_{PQ}^\dagger\mathbf{X}_{QP} = \mathbf{A}_{PP} = \mathbf{T}_{PP}\mathbf{D}_P^2\mathbf{T}_{PP}^\dagger$, $(\mathbf{T}_{PP}^\dagger = \mathbf{T}_{PP}^{-1})$.
(8) Calculate $\mathbf{U}_{PP}$ and $\mathbf{V}_{PP}$.
(9) Calculate $(\mathbf{CHXV})_{PP} = (\mathbf{CHX})_{PP}\mathbf{V}_{PP}$, $\mathbf{Y}_{PP}$, and $\mathbf{Z}_{MP}$.
(10) Diagonalize the GVVPT3 effective Hamiltonian matrix $(\mathbf{H}_U^{\text{eff}})_{MM}$, which is not explicitly constructed, using Davidson's method with $\boldsymbol{\sigma}$ vectors as in eq 36.

IV. Test Calculations and Discussion

Calculations for some representative molecules with different model and external spaces using three GVVPT2 codes were performed, and the computation times are given in Table 1. Only one primary state, i.e., $N_p = 1$, is considered in all cases except that two primary states ($N_p = 2$) are calculated for the c-C_4H_4 molecule. The sizes of the model spaces (N_m) and total spaces ($N = N_m + N_q$) are also given in terms of numbers of CSFs. Three algorithms, CFGCI, Table-CI, and conventional CSF-based GUGA-CI, were compared. As we expected, the relative speed of the three different codes is CFGCI > GUGA-CI > Table-CI, which is the same as the corresponding MRCISD speeds. The CFGCI-based GVVPT2 is about 30 times faster than the Table-CI version for small cases. The speed-up is more significant for larger molecular systems, especially for larger model spaces. The computation times by GVVPT3 codes are about one iteration of their parent CI methods. CFGCI-based GVVPT3 is 5−11 times faster than the conventional GUGA-CI counterpart in our test calculations.

The high efficiency of the new GVVPT2 code allows accurate theoretical study of larger molecular systems at low cost. The study of the ground state of c-C_4H_4 by GVVPT2 is used as an illustration. The stable geometry of the ground state of c-C_4H_4 is a planar rectangle, as confirmed by many experiments (see,

TABLE 1: Wall Times (Seconds) of Three GVVPT2 Codes and Two GVVPT3 Codes[a]

molecule	NO^-	NO^-	N_2	c-C_4H_4[b]	NiO_2
model CSFs	96	96	176	3 094	3 420
total CSFs	7 529 132	23 142 808	3 253 114	329 114 892	3 784 597 999
Table-CI	27	124	17	14 368	
GUGA-CI	7	63	4	9 259	24 216
CFGCI	1	4	<1	73	611
speed-up[c]	27	31		197	
GUGA-CI(3)	11 130		502		
CFGCI(3)	941		111		

[a] Table-CI, GUGA-CI, and CFGCI indicate the corresponding GVVPT codes based in Table-CI, conventional GUGA-CI, and CFGCI, respectively. Three in parentheses represents GVVPT3; otherwise, the method is GVVPT2. One primary state is considered unless specified otherwise. [b] Cyclobutadiene using the cc-pVDZ basis set. Two primary states are considered. [c] The ratio of GVVPT2 speeds based on a CFGCI- and Table-CI-based algorithm.

TABLE 2: Optimized Structure of Cyclobutadiene by GVVPT2 Using the cc-pVTZ Basis Set (Bond Lengths Are in Angstroms, and Bond Angles Are in Degrees)

geometry	method	R(C═C)	R(C—C)	R(C—H)	HCC
	Basis Set: cc-pVDZ				
rectangle	GVVPT2	1.372	1.574	1.095	134.88
	MRCCSD(T)[a]	1.370	1.575	1.095	134.87
	MRAQCC[b]	1.367	1.573	1.093	134.9
square	GVVPT2		1.464	1.094	135.0
	MRCCSD(T)[a]		1.465	1.094	135.0
	MRAQCC[b]		1.463	1.090	135.0
	Basis Set: cc-pVTZ				
rectangle	GVVPT2	1.355	1.565	1.080	134.9
	MRCCSD(T)[a]	1.354	1.564	1.079	134.9
	MRAQCC[b]	1.349	1.562	1.077	134.9
square	GVVPT2		1.450	1.079	135.0
	MRCCSD(T)[a]		1.451	1.078	135.0
	MRAQCC[b]		1.447	1.076	135.0

[a] From ref 24. [b] From ref 18.

e.g., ref 22). It can automerize between two equivalent D_{2h} structures through a square intermediate. The automerization reaction has been studied theoretically by highly accurate MRCC[23,24] and MRAQCC methods.[18] In a GVVPT2 study, the choice of model space is critical, as it is in the optimization of molecular orbitals in the preceding MCSCF. In the study of c-C_4H_4, the four lowest molecular orbitals ($1a_g$, $1b_{1g}$, $1b_{2u}$, $1b_{3u}$) are taken as the core (i.e., doubly occupied in all configurations of the MCSCF). The valence orbitals are divided into five groups: ($2a_g$, $2b_{1g}$, $2b_{2u}$, $2b_{3u}$) for σ_{CH}; ($3a_g$, $4a_g$, $3b_{2u}$, $3b_{3u}$) for σ_{CC}; ($3b_{1g}$, $4b_{1g}$, $4b_{2u}$, $4b_{3u}$) for σ^*_{CC}; ($5a_g$, $5b_{1g}$, $5b_{2u}$, $5b_{3u}$) for σ^*_{CH}; and ($1b_{2g}$, $1b_{3g}$, $1a_u$, $1b_{1u}$) for $\pi_{CC}\pi^*_{CC}$. The major configurations include four electrons and four orbitals in $\pi_{CC}\pi^*_{CC}$ and full occupancies in σ_{CH} and σ_{CC}. Single and double excitations from σ_{CH} to σ^*_{CH} and from σ_{CC} to σ^*_{CC} are considered while keeping four electrons in $\pi_{CC}\pi^*_{CC}$. Up to quadruple excitations from σ_{CH} or σ_{CC} to $\pi_{CC}\pi^*_{CC}$, or from $\pi_{CC}\pi^*_{CC}$ to σ^*_{CH} or σ^*_{CC}, are also included. The configurations in this model space generate 3094 CSFs. We use such a relatively large model space to demonstrate the efficiency of the new GVVPT2 code and to test the effectiveness of GVVPT2 in recovering electron correlation relative to the highly accurate MRCCSD(T) and MRAQCC. The molecular orbitals were optimized for the two lowest singlet states (^1A_g) using state-averaged (SA) MCSCF with equal weights of both states. Two primary states were considered in all GVVPT calculations. The geometry optimization was based on the energy of the ground state. When the cc-pVTZ basis set is used, the total space includes 2 389 313 884 CSFs. Despite its size, the GVVPT2 part of a single point calculation required only 314 s on a 2.0 GHz dual core AMD Opteron Processor 2212. As shown in Table 2, our prediction of geometry is in excellent agreement with MRCCSD(T). The autmerization energy barrier predicted by GVVPT2 is 7.7 kcal/mol, which is close to the 8.6 kcal/mol predicted by the MRAQCC method.[18]

V. Conclusions

In conclusion, a new GVVPT2 code based on a configuration-driven graphical unitary group approach CI code (CFGCI) has been implemented and proved to be much more efficient than the previous version that was based in Table-CI. The efficiency of the new algorithm was illustrated by calculations on a set of model compounds and on cyclobutadiene; speed-ups of 1−2 orders of magnitude have been realized. Geometrical parameters of both the equilibrium and automerization transition structures of the conjugated organic molecule cyclobutadiene by the GVVPT2 method are in close agreement with MRCCSD(T) and MRAQCC results. The prediction of the energy barrier to automerization is also in good agreement with MRAQCC. With this new CFGCI-based code, GVVPT2 can now be used to study larger systems, including transition states of organic molecules. GVVPT2 is seen to continue to be a very promising method in quantum chemistry, and is shown in this study to be amenable to algorithmic advances that allow it to be applied to challenging molecules of larger size than previously possible.

Acknowledgment. We thank Alexander V. Gaenko for results using his GVVPT3 code based on CSF-driven GUGA-CI. The authors gratefully acknowledge the Department of Energy Office of Science under Award Number DE-FG02-06ER46292 for financial support.

References and Notes

(1) Hoffmann, M. R. *J. Phys. Chem.* **1996**, *100*, 6125–6130.
(2) Khait, Y. G.; Hoffmann, M. R. *J. Chem. Phys.* **1998**, *108*, 8317–8330.
(3) Khait, Y. G.; Song, J.; Hoffmann, M. R. *J. Chem. Phys.* **2002**, *117*, 4133–4145.
(4) Song, J.; Khait, Y. G.; Wang, H.; Hoffmann, M. R. *J. Chem. Phys.* **2003**, *118*, 10065–10072.
(5) Devarajan, A.; Gaenko, A. V.; Khait, Y. G.; Hoffmann, M. R. *J. Phys. Chem. A* **2008**, *112*, 2677–2682.
(6) Buenker, R. J.; Krebs, S. In *Recent Advances in Multireference Methods*; Hirao, K., Ed.; World Scientific: Singapore, 1999; Vol. 4, pp 1−29.
(7) Khait, Y. G.; Hoffmann, M. R. In *Low-lying Potential Energy Surfaces*; Hoffmann, M. R., Dyall, K. G., Eds.; ACS Symposium Series 828; American Chemical Society: Washington, DC, 2002; pp 329−345.
(8) Paldus, J. *J. Chem. Phys.* **1974**, *61*, 5321–5330.
(9) Paldus, J.; Boyle, M. J. *Phys. Scr.* **1980**, *21*, 295–311.
(10) Paldus, J. Unitary Group Approach to Many-electron Correlation Problem. In *The Unitary Group for the Evaluation of Electronic Energy Matrix Elements*; Hinze, J., Ed.; Lecture Notes in Chemistry, Vol. 22; Springer: Berlin, 1981; pp 1−50.

(11) Paldus, J. Lie Algebraic Approach to the Many-Electron Correlation Problem. In *Mathematical Frontiers in Computational Chemical Physics*; Truhlar, D. G., Ed.; Springer: New York, 1988; pp 262−299.

(12) Shavitt, I. The Graphical Unitary Group Approach and its Application to Direct Configuration Interaction Calculations. In *The Unitary Group for the Evaluation of Electronic Energy Matrix Elements*; Hinze, J., Ed.; Lecture Notes in Chemistry, Vol. 22; Springer: Berlin, 1981; pp 51−99.

(13) Shavitt, I. Unitary Group Approach to Configuration Interaction Calculations of the Electronic Structure of Atoms and Molecules. In *Mathematical Frontiers in Computational Chemical Physics*; Truhlar, D. G., Ed.; Springer: New York, 1988; pp 300−349.

(14) Brooks, B. R.; Schaefer, H. F., III. *J. Chem. Phys.* **1979**, *70*, 5092–5106.

(15) Jiang, W.; Khait, Y. G.; Hoffmann, M. R. In preparation.

(16) Khait, Y. G.; Hoffmann, M. R. *Int. J. Quantum Chem.* **2004**, *99*, 210–220.

(17) Jiang, W.; Khait, Y. G.; Hoffmann, M. R. *THEOCHEM* **2006**, *771*, 73–78.

(18) Echert-Maksic, M.; Vazdar, M.; Barbatti, M.; Lischka, H.; Maksic, Z. B. *J. Chem. Phys.* **2006**, *125*, 064310.

(19) Malrieu, J. P.; Durand, Ph.; Daudey, J. P. *J. Phys. A: Math. Gen.* **1985**, *18*, 809–826.

(20) Davidson, E. R. *J. Comput. Phys.* **1975**, *17*, 87–94.

(21) Siegbahn, P. E. M. Factorization of the Direct CI Coupling Coefficients into Internal and External Parts. In *The Unitary Group for the Evaluation of Electronic Energy Matrix Elements*; Hinze, J., Ed.; Lecture Notes in Chemistry, Vol. 22; Springer: Berlin, 1981; pp 119−135.

(22) Irngartinger, H.; Nixdorf, M. *Angew. Chem., Int. Ed. Engl.* **1983**, *22*, 403–404.

(23) Balkova, A.; Bartlett, R. J. *J. Chem. Phys.* **1994**, *101*, 8972–8987.

(24) Demel, O.; Pittner, J. *J. Chem. Phys.* **2006**, *124*, 144112.

JP811082P